



Distal conformational locks on ferrocene mechanophores guide reaction pathways for increased mechanochemical reactivity

Yudi Zhang 1, Zi Wang 1, Tatiana B. Kouznetsova 1, Ye Sha 2, Enhua Xu4, Logan Shannahan5, Muge Fermen-Coker⁵, Yangju Lin[®]¹, Chuanbing Tang[®]² and Stephen L. Craig[®]¹

■

Mechanophores can be used to produce strain-dependent covalent chemical responses in polymeric materials, including stress strengthening, stress sensing and network remodelling. In general, it is desirable for mechanophores to be inert in the absence of force but highly reactive under applied tension. Metallocenes possess potentially useful combinations of force-free stability and force-coupled reactivity, but the mechanistic basis of this reactivity remains largely unexplored. Here, we have used single-molecule force spectroscopy to show that the mechanical reactivities of a series of ferrocenophanes are not correlated with ring strain in the reactants, but with the extent of rotational alignment of their two cyclopentadienyl ligands. Distal attachments can be used to restrict the mechanism of ferrocene dissociation to proceed through ligand 'peeling', as opposed to the more conventional 'shearing' mechanism of the parent ferrocene, leading the dissociation rate constant to increase by several orders of magnitude at forces of ~1 nN. It also leads to improved macroscopic, multi-responsive behaviour, including mechanochromism and force-induced cross-linking in ferrocenophane-containing polymers.

key concept of polymer mechanochemistry is to trigger transformations within a polymer through the manipulation of force-sensitive functional groups (mechanophores)^{1,2}. Covalent polymer mechanochemistry holds great promise through two approaches: using stress transfer in strained polymers to alter reaction pathways and obtain products that are otherwise difficult or impossible to access³⁻⁵, and using mechanically coupled chemistry to drive changes in the properties and functions of polymers, including stress sensing⁶⁻¹⁰, self-strengthening¹¹⁻¹³ and the conversion of electronic properties¹⁴. Practical applications of covalent mechanochemistry in materials, however, are often limited by low levels of activity. The low levels of activity are exacerbated by the simultaneous desire for mechanophores to be inert in the absence of force.

Recent studies have shown that metallocenes display significant mechanical activity despite being highly inert15-17. For example, the Fe-cyclopentadienyl (Cp) bond (bond dissociation energy (BDE) is up to 90 kcal mol-1) has a mechanical strength that under conditions of pulsed sonication is phenomenologically similar to that of the carbon-nitrogen bond of azobisdialkylnitrile (BDE < 30 kcal mol⁻¹)¹⁵. These observations have motivated us to further investigate the mechanical reactivity of metallocenes, to increase their mechanochemical activity while retaining their force-free inertness. Of particular interest is the relationship between mechanical lability and the mechanism of metalligand dissociation. When metallocenes are stretched, their initial conformational response is rotation around the central ligandmetal-ligand (L-M-L) axis so that the two Cp ligand attachments have a dihedral angle of ~180°, that is, opposite to each other. Further increasing the force induces a 'shearing' or sliding dissociation motion of the labile Cp ligands (Fig. 1a). Because mechanochemical coupling depends on the reaction pathway, we wondered whether alternative pathways might display substantially different mechanical labilities.

We reasoned that judicious placement of ansa-bridging substituents (that is, Cp ligands connected by a bridge) could 'lock' the initial Cp rotation and steer Cp ligand dissociation into a 'peeling' pathway (Fig. 1b). Here, the mechanical reactivity of ansa-bridged ferrocenes (ferrocenophanes, FCPs) has been quantified using single-molecule force spectroscopy (SMFS), which revealed that conformational restriction through distal attachment greatly influences the mechanochemical reactivity. Specifically, the conformational freedom of unbridged ferrocene actually reduces its mechanochemical activity by driving Cp dissociation into a less active 'shearing' pathway. By contrast, conformational restriction in FCPs can be used to direct Cp dissociation into a 'peeling' pathway that increases the rate constant of force-coupled dissociation by several orders of magnitude. The resulting mechanochemical reactivity of FCPs was subsequently exploited to improve colourimetric and network structure changes in bulk materials.

Results and discussion

Our strategy was to synthesize multi-mechanophore-containing polymers and characterize their mechanochemical reactivity by SMFS (Fig. 2). Three FCP diene derivatives were incorporated into copolymers (number-averaged molecular mass, $M_n = 115$, 96 and 108 kDa for cis-[3]ferrocenophane (cis-3FCP), trans-[3]ferrocenophane (trans-3FCP) and cis-[5] ferrocenophane (cis-5FCP), respectively) through entropy-driven ring-opening metathesis polymerization (ED-ROMP)¹⁸ of the appropriate macrocyclic monomer with 9-oxabicyclo [6.1.0] non-4-ene (epoxy-COD; Fig. 2a). Epoxy-COD was employed as co-monomer to increase the adhesion

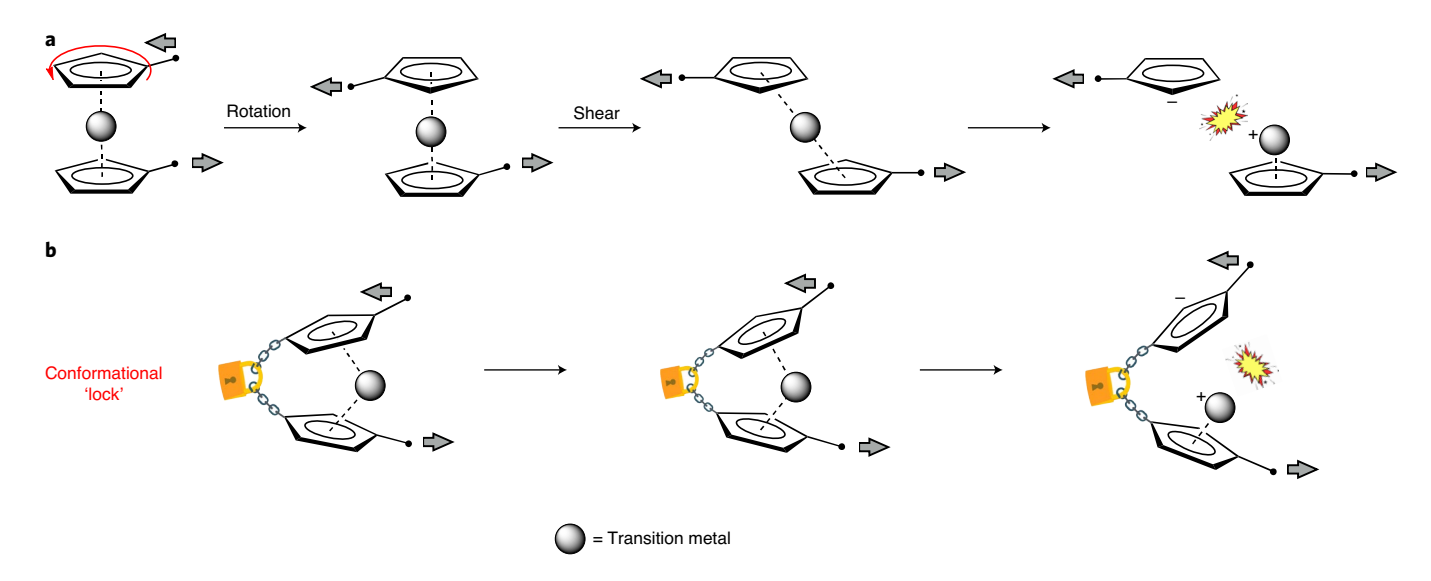


Fig. 1 | Schematic illustration of the proposed mechanochemical dissociation mechanisms and their relationship to metallocene structure. **a**, Shearing of unconstrained metallocenes. **b**, Peeling of conformationally locked metallocenophanes. The structures shown here are merely to communicate snapshots along a force-coupled reaction pathway and they are not necessarily true intermediates. Some of the steps may be reversible depending on the magnitude of the force.

of polymers to the cantilever tips employed in atomic force microscopy (AFM), as described previously¹⁸.

Single-molecule force spectroscopy. In the SMFS study, constant velocity and force clamping experiments were combined to access a wider range of force¹⁹⁻²². In the constant velocity experiments, the rupture of the Fe-Cp bond released the stored bridge length, which resulted in a characteristic plateau in the force-separation curves (Fig. 2b). In the force clamping experiments²², the polymer chain was trapped between the AFM tip and the surface under a constant force while the elongation of the polymer was measured as a function of time (Supplementary Figs. 3 and 4). The changes in polymer contour length were obtained by fitting the pre- and post-transition force curves in the constant velocity experiments to an extended, freely jointed chain model²³. The experimental changes in contour length agreed well with the constrained geometry simulates external force²⁴ (CoGEF) simulation results (Supplementary Table 14 and Supplementary Fig. 10), and the polymer extension was proportional to FCP content in the backbone (Supplementary Fig. 10), indicating the quantitative rupture of FCP units along the polymer backbone and a negligible contribution from the partial rupture of any 'double tethers' (Supplementary Fig. 11).

Surprisingly, as shown in Fig. 2b, the threshold force for *cis*-3FCP opening is only $800 \pm 25 \,\mathrm{pN}$; at this force, the effective unimolecular rate constant for Cp dissociation is 24 s⁻¹, which is roughly a factor of 1018 greater than that of the force-free reaction (see below). To directly compare its activity with unbridged ferrocene, we employed a common reference: the mechanochemical ring opening of a [4.2.0] bicyclooctene (BCOE) mechanophore²⁵. When BCOE ring opening was probed by SMFS under identical conditions to those employed for cis-3FCP, the transition force was found to be ~1,620 pN, or more than 800 pN greater than that of cis-3FCP. Extrapolation of the force-rate behaviour to 1,250 pN gave a force-coupled rate constant of 2.4×10^{-2} s⁻¹ (Supplementary Section 5.4). The relative mechanochemical activity of unbridged ferrocene and BCOE was determined by the sonication of a random ferrocene-co-BCOE copolymer. Here, the two mechanochemical reactions are in direct competition, and a greater extent of BCOE ring opening (5% activation) than ferrocene scission (2% activation) was observed (Supplementary Fig. 1).

As for previous studies²⁶, the forces that dominate the sonochemical responses were larger than those involved in the SMFS studies. Because ferrocene dissociation is slower than BCOE ring opening at zero force and also slower than BCOE ring opening at higher force, we conclude that it is slower as well at the forces involved in the SMFS experiments, a conclusion qualitatively supported by an analvsis of force-coupled strand-breaking of ferrocene-containing polymers (Supplementary Section 5.1). Therefore, the analogous SMFS transition force for ferrocene dissociation is >1,600 pN, and Cp dissociation from cis-3FCP is ~107 (or more) times faster than from unbridged ferrocene at the high force of ~1,250 pN, a difference in reactivity not seen in the corresponding low and/or force-free reactions. The faster dissociation of Cp at high forces in cis-3FCP cannot be attributed solely to its ring strain, as previous reports indicate that the ring strain in cis-3FCP is only 2.8 kcal mol⁻¹. Thus, even if that ring strain were completely relieved in the transition state for Cp dissociation (that is, if the barrier to dissociation were 2.8 kcal mol-1 lower), the effect of ring strain would be far too small to account for seven orders of magnitude difference in reactivity (Supplementary Table 8).

We therefore considered that the increased mechanochemical reactivity of *cis-*3FCP relative to the unbridged ferrocene is largely due to a change in mechanism (and associated mechanical coupling) enforced by the placement of the bridge. To test this hypothesis, two additional mechanophores were synthesized: cis-5FCP, which has minimal ring strain (~0.7 kcal mol-1, Supplementary Table 8) but a similar bridge position to cis-3FCP, and trans-3FCP, which has very similar ring strain (~2.8 kcal mol⁻¹) to cis-3FCP but a different bridge position. Figure 2b shows that the threshold force is $960 \pm 34 \,\mathrm{pN}$ for *cis-*5FCP and $1,140 \pm 30 \,\mathrm{pN}$ for *trans-*3FCP. At a force of 1,250 pN, the dissociation rate constant for cis-5FCP is 8.1×10^3 s⁻¹ (extrapolation from the force-rate behaviour in Fig. 2c, see details in Supplementary Fig. 5) whereas for trans-3FCP it is only 2 s⁻¹ (Fig. 2c). It is therefore the position of the bridge, rather than the strain the bridge introduces, that is the predominant determinant of mechanochemical activity.

Calculations and reaction path analysis. To obtain a clear picture of the dissociation mechanisms of the FCPs and ferrocene under

NATURE CHEMISTRY ARTICLES

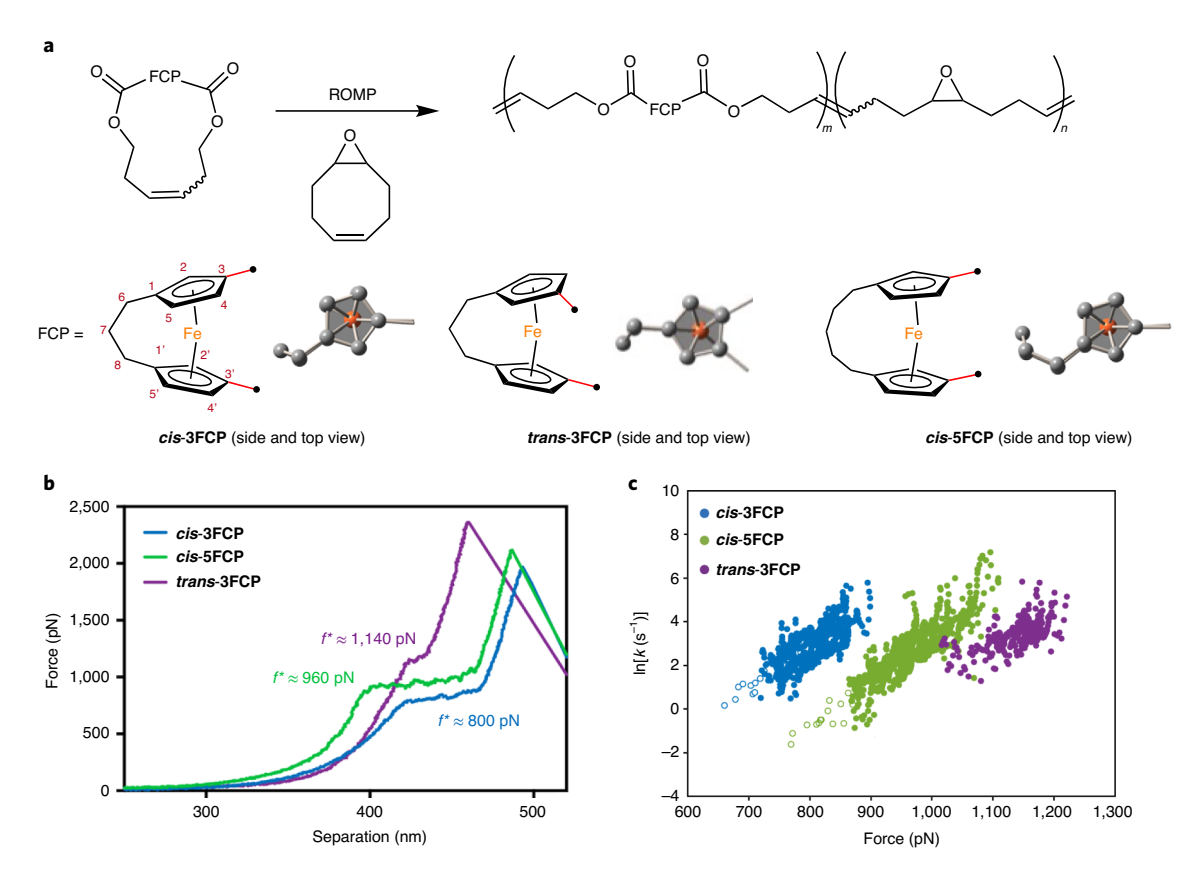


Fig. 2 | FCP polymers used in this study and their respective behaviour in SMFS experiments. **a**, Synthesis of the polymers involved copolymerization of the *cis*-3FCP, *trans*-3FCP or *cis*-5FCP macrocycle with epoxy-COD by ROMP. **b**, Representative single-molecule force-extension curves of copolymers containing 18% *cis*-3FCP, 30% *cis*-5FCP and 7% *trans*-3FCP. The f^* values correspond to the average value of the midpoint of the plateau of the multiple force-extension curves (tip velocity = 300 nm s⁻¹). **c**, Rate-force relationships for *cis*-3FCP, *cis*-5FCP and *trans*-3FCP, plotted as In-linear graphs. The empty blue and green circles were obtained from force clamping experiments (Supplementary Section 5.2); the filled circles were obtained from constant velocity experiments.

force, density functional theory (DFT) simulations were performed with a CoGEF method. The two terminal atoms of the monomers were moved apart in a stepwise fashion and the structures were minimized to mimic a quasi-static mechanochemical experiment. The structural evolution of the four mechanophores as a function of strain is shown in Fig. 3b. We chose the displacement from the intersection point of the surface normal of the first Cp and the second Cp to the mass centre of the second Cp as a parameter to define the dissociation mechanisms. A peeling mechanism moves the top Cp plane to the right (plus sign) while a shearing mechanism moves it to the left (minus sign; Supplementary Fig. 15). In addition, the projected dihedral angles of the initially parallel Cp rings (β) and the dihedral angles of the initially eclipsing side-chain attachment points (α) are especially informative and are shown in Fig. 3a,c (for further details, see Supplementary Figs. 16 and 17). Interestingly, the grouping of the observed mechanical reactivity is maintained in the structural snapshots. For the more reactive cis-3FCP and cis-5FCP mechanophores, the eclipsing angle between the two side chains remains close to 0° until the Fe-Cp bond breaks while the dihedral angle between Cp rings increases steadily, indicating no relative rotation of the Cp rings but a gradual 'peeling' of one away from the other. By contrast, for the less mechanically reactive trans-3FCP and unbridged ferrocene (FC), the opposite is observed: with increasing stretch distance, the angle between the side chains increases while the two Cp ligands maintain a much more parallel alignment (particularly in the unbridged ferrocene). As seen in the snapshots in Fig. 3b, ferrocene dissociates through a purely 'shearing' pathway that is triggered by the initial rotation of the Cp rings at a force of ~40 pN (Supplementary Fig. 14) to produce oppositely positioned pulling points, whereas the modest increase in the plane–plane angle for *trans-3FCP* before rupture suggests a combination of shearing and peeling.

The change in mechanism, quantified by the projections in Fig. 3b, is dictated at the molecular level by the structural restriction on side-chain reorientation (α) imposed by the *ansa* bridges. The correlation between the side-chain angle at the point of ligand dissociation and the SMFS plateau force is shown graphically in Fig. 4. Qualitatively, the dissociation force increases (mechanochemical reactivity decreases) with the force-coupled increase in side-chain angle that is permitted by the ansa bridges. Additional simulations on the effect of peeling on ferrocene dissociation were performed by fixing the side-chain angle of a ferrocene monomer to 0° to enforce an eclipsed geometry in the absence of an ansa bridge. Consistent with our interpretation, the computationally enforced peeling of ferrocene results in much smaller maximum forces and dissociation energies (Supplementary Fig. 14 and Supplementary Table 17) than are observed in the unconstrained shearing pathway. The data and discussion can be found in the Supplementary Information. The above evidence supports peeling as the mechanically favoured pathway for bridged ferrocene.

An unusual feature of the observed reactivity is that the conformationally restricted reactants access a more favoured pathway than the reactants that are initially unrestricted, an almost uniquely mechanical effect that results directly from the fact that the applied mechanical force literally pulls the unconstrained ferrocene into a less mechanically reactive conformation. The mechanical steering

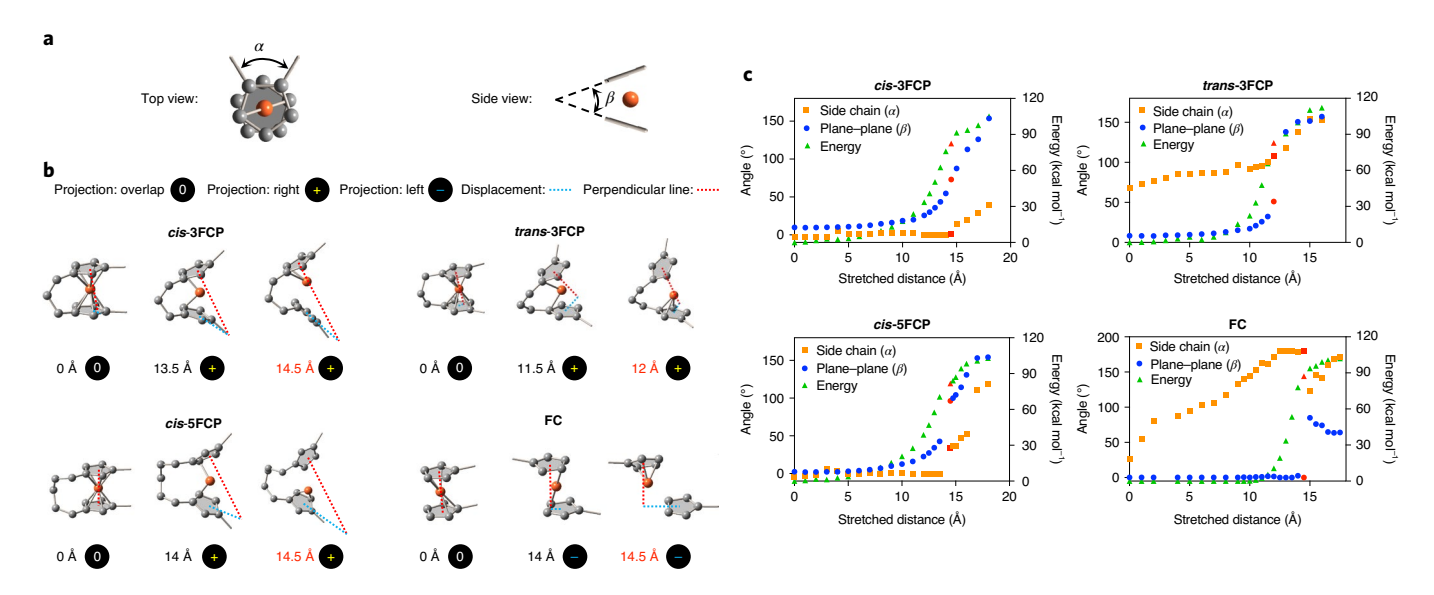


Fig. 3 | The relationship between FCP structure and the structural changes that accompany ligand dissociation. **a**, Illustration of the side-chain dihedral angle (α) and the plane-plane dihedral angle (β). **b**, Structural evolution of *cis*-3FCP, *trans*-3FCP, *cis*-5FCP and FC as a function of linear displacement of the chain attachment points (not shown here). **c**, The overall calculated strain energy and β and α angles as a function of displacement for *cis*-3FCP, *trans*-3FCP, *cis*-5FCP and FC. The data points corresponding to metal-ligand dissociation are marked in red.

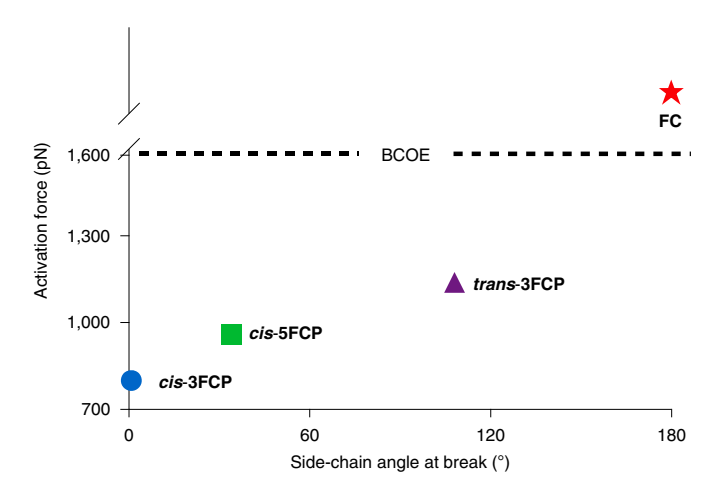


Fig. 4 | Correlation between side-chain angle at ligand dissociation and the SMFS plateau force. The correlation between side-chain angle at break and activation force (timescale of 0.1s) for *cis-*3FCP, *cis-*5FCP, *trans-*3FCP and FC. The break in the *y* axis indicates that the exact activation force for FC is not known, but ligand dissociation in FC has been shown to require higher forces than are involved in the ring opening of BCOE $(-1.6 \, \text{nN})^{25}$. The apparent linear alignment of the four points is therefore artificial.

of a reactant into less reactive conformations and pathways is reminiscent of the 'catch bond'-like behaviour that has been observed in biological systems such as the mechanical separation of DNA 27 or β -strands in proteins 28 . In synthetic chemical systems, numerous theoretical studies have shown how pulling geometry can have significant effects on reaction pathways and mechanochemical reactivity $^{29-32}$, but the force-coupled reactivity differences best exemplified by $\emph{cis-3FCP}$ and ferrocene are subtly but importantly different from previous examples. In this system, the difference in coupling is not due to differences in the initial regio- or stereochemistry of the pulling attachments, which are essentially the same across the series of mechanophores. Instead, the increased reactivity in $\emph{cis-3FCP}$ results from the addition of a conformational restraint that is distal

Table 1 | Ligand dissociation rate constants and activation lengths for the FCP mechanophores

	k_0^a (s ⁻¹)	Δx^{\ddagger} (cusp $^{ extsf{b}}$) (Å)	Δx^{\ddagger} (computed ^c) (Å)
cis-3FCP	3×10^{-17}	2.55 ± 0.08	3.02 ± 0.12
trans-3FCP	3×10^{-17}	1.84 ± 0.03	2.16 ± 0.17
cis-5FCP	1×10^{-18}	2.35 ± 0.06	2.85 ± 0.15

 $^{\circ}$ The values of k_0 at room temperature were estimated from the activation energy of the isomerization/decomposition kinetics at 220 $^{\circ}$ C (Supplementary Figs. 6 and 7 and Supplementary Table 9). $^{\circ}$ The uncertainties in the cusp fit do not account for the uncertainty in k_0 (Supplementary Table 15). $^{\circ}$ The difference in X--X distance in the ground state compared with the transition state (last CoGEF structure before ligand dissociation).

to the pulling points and serves to guide what is effectively the same initial pulling geometry into a desired pathway.

The mechanochemical coupling that results from this conformational locking is substantial. Force-free rate constants for Cp dissociation were estimated from isomerization kinetics to be in the neighbourhood of 10^{-17} s⁻¹ (Table 1), as follows. The rate constant for cis-to-trans **3FCP** isomerization/decomposition at 220 °C was measured to be 2×10^{-5} s⁻¹, corresponding to the Gibbs energy of activation $\Delta G^{\ddagger}(493 \text{ K}) = 40 \text{ kcal mol}^{-1}$. If the entropy of activation $\Delta S^{\ddagger} = 0$, then $\Delta G^{\ddagger}(298 \text{ K}) = 40 \text{ kcal mol}^{-1}$ and the corresponding rate constant is 3×10^{-17} s⁻¹. In practice, ΔS^{\ddagger} is likely to be slightly positive, but by less than the entropy for the ring opening of five- or six-membered rings (~10 cal K⁻¹ mol⁻¹)³³. Thus, $\Delta G^{\ddagger}(298 \text{ K}) = 40 \text{ kcal mol}^{-1}$ is likely to be an underestimate, the rate constant of $10^{-17} \, \mathrm{s}^{-1}$ is likely to be a slight overestimate, and so forces of 1 nN lead to rate constant increases of up to 20 orders of magnitude. This force dependence is not the result of Bell-Evans-type coupling, which assumes a constant exponential dependence of the rate constant on force, as expressed by equation (1)^{34,35}. Here, k(F) is the force-coupled rate constant, k_0 is the force-free rate constant, F is force, $k_{\rm B}$ is Boltzmann's constant, T is temperature and Δx^{\ddagger} corresponds to the change in polymer contour length as the mechanophore goes from the ground state to the transition state and indicates the efficiency of mechanochemical coupling. An Eyring extrapolation of the rate constant versus force data NATURE CHEMISTRY ARTICLES

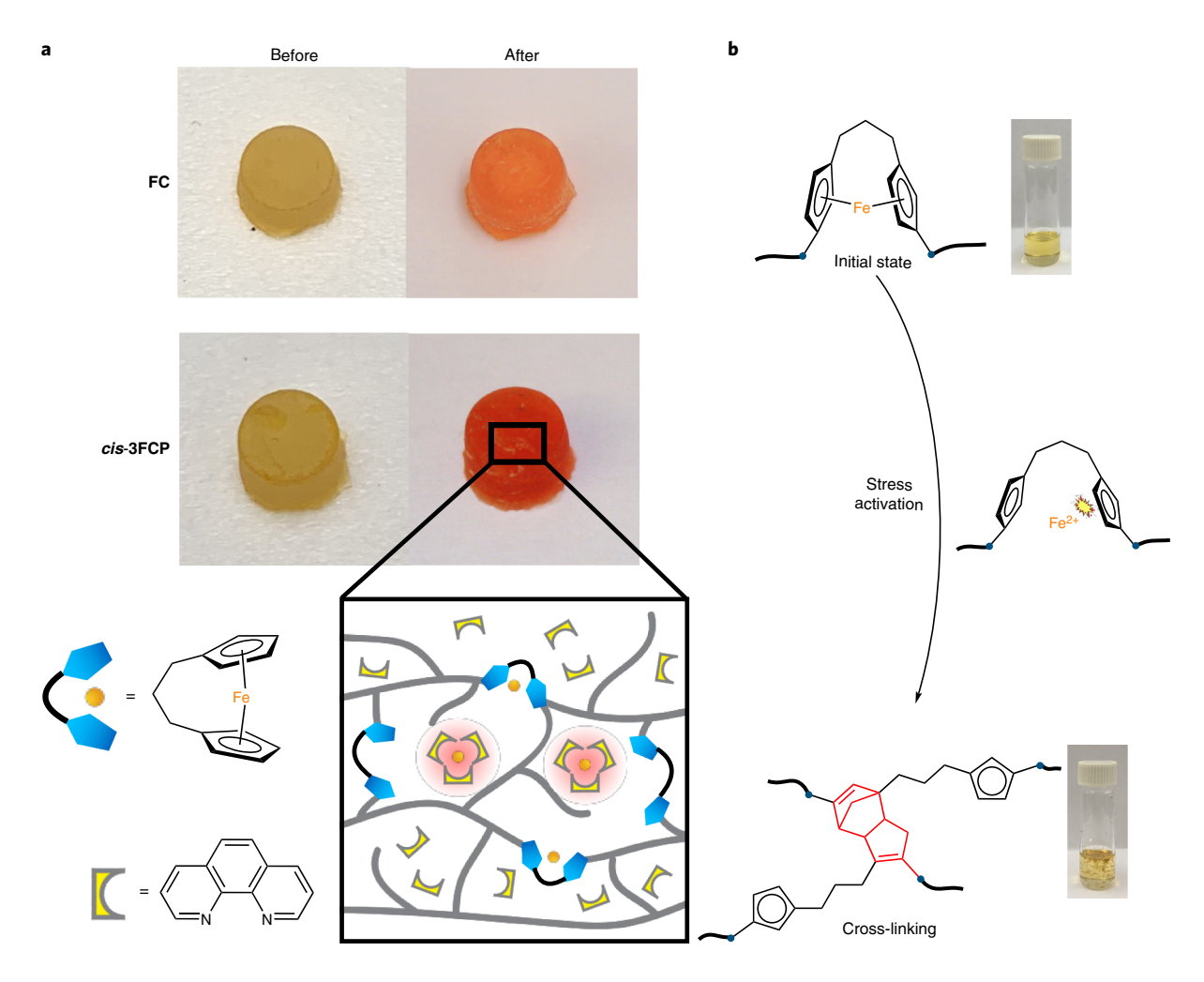


Fig. 5 | Multifunctional mechanochemical responses of *cis***-3FCP. a,** Schematic illustration of phenanthroline capturing liberated Fe²⁺ within a bulk material and photographs of a polydimethylsiloxane plug with covalently embedded ferrocene (top) and *cis***-3FCP** (bottom) before (left) and after (right) the drop test. **b,** Schematic illustration of the *cis*-3FCP-containing polymer before sonication (top) and cross-linking by the Diels-Alder reaction (or dimerization) between Cp units after activation (bottom) and photographs of the *cis*-3FCP-containing polymer completely dissolved in DCM before sonication (top) and insoluble precipitates in DCM after sonication for 30 min (bottom).

presented in Fig. 2c gives force-free rate constants (Supplementary Table 7) that are 10 to 11 orders of magnitude higher than the experimental results (Supplementary Table 9). By comparison, fitting with a potential energy that is a truncated quadratic (cusp model, equation (2))36-38, which accounts for changes in the shape of the potential energy surface, including the position of the transition state, yields Δx^{\dagger} values that are in reasonable agreement with the structural evolution captured by CoGEF simulation (within experimental uncertainty; Supplementary Table 15). Although the cusp energy surface is undoubtedly an oversimplified model of the reaction, especially given the large changes in geometry, it allows us to approximate differences in geometric changes among the reactions. The fact that the force-coupled dissociation rate constant fits better with the cusp model indicates that the relative position of the reactant and transition state changes substantially as a function of force, consistent with the large reactant distortions that are observed in the simulations prior to dissociation (Fig. 3b,c). In addition, both the SMFS analysis and the computational results (Table 1) show that the mechanical couplings (Δx^{\ddagger}) are large and the peeling pathway of *cis*-3FCP is the best coupled (highest Δx^{\ddagger}) among the three, whereas the greater shearing character in trans-3FCP leads to the worst coupling (lowest Δx^{\ddagger}).

$$k(F) = k_0 e^{F\Delta x^{\dagger}/k_B T} \tag{1}$$

$$k(F) = k_0 \left(1 - \frac{F \Delta x^{\ddagger}}{2 \Delta G^{\ddagger}} \right) e^{F \Delta x^{\ddagger}/k_B T - \left(F^{\ddagger} \Delta x^{\ddagger}\right)^2 / 4 \Delta G^{\ddagger} k_B T}$$
 (2)

Activity in bulk materials. These mechanistic factors influence the stress-responsive behaviour in bulk materials. We incorporated *cis-3FCP* and ferrocene as stress-bearing, covalent cross-links into silicone elastomers (Sylgard 184, Fig. 5a) following previously reported methods (Supplementary Section 1.5)^{39,40}. Phenanthroline was used as a trap for released Fe²⁺, and was introduced into the cured elastomer by swelling in dichloromethane (DCM), which was subsequently removed by evaporation. The otherwise identical plugs of mechanophore-containing elastomers were subjected to two high-strain rate impact tests: a drop test in which a weight was released from a fixed height (Supplementary Fig. 20), and a split Hopkinson pressure bar test. As seen in Fig. 5a and Supplementary Fig. 22, in both cases the *cis-3FCP* specimen developed a deeper red colour following impact than the specimen with ferrocene. To quantify their mechanochromic responses, UV-Vis

spectra of the silicone specimens were obtained before and after the drop test. The red colour and absorption spectra ($\lambda_{\text{max}} \approx 520 \text{ nm}$, Supplementary Figs. 21 and 24) of the activated materials are consistent with those reported previously⁴¹ for the expected formation of a [Fe(phenanthroline)₃]²⁺ complex. The fraction of *cis-*3FCP activated in the drop test was ~1%, whereas the fraction of ferrocene activated was ~0.4% (Supplementary Section 8.2). Notably, this colour change was irreversible under ambient conditions, although still providing a colourimetric indication of strain that is comparable to that generated by other mechanochromic, but reversible, force probes such as spiropyran³⁹ and naphthopyran derivatives⁴⁰. The qualitatively stronger bulk mechanochromic response of cis-3FCP compared with ferrocene is attributed to the distal attachment of the conformationally restrictive ansa bridge and enforced peeling dissociation mechanism, as discussed above. In addition, a different colourimetric response can be achieved by using a different exogenous ligand. For example, the specimen developed a dark brownish colour when ligand 2,4,6-tris(2-pyridyl)-s-triazine was used instead of phenanthroline (Supplementary Fig. 25).

architectures hold additional promise The FCP stress-responsive cross-linking. We sonicated a *cis-3FCP*-containing polymer (cis-3FCP-co-gem-dichlorocyclopropane, 10% FCP molar ratio) and observed that polymeric precipitates were formed over the course of 30 minutes. This behaviour is reminiscent of that observed in stress-responsive cross-linking systems^{11,42,43}, with cross-linking further supported by the inability to dissolve the precipitate in any of the numerous solvents tried (Fig. 5b). By comparison, no cross-linking was observed for ferrocene-containing polymers under the same conditions¹⁵. Several pieces of evidence suggest that the cross-linking occurs mainly through the liberated Cp ligands (Cp is prone to dimerization). First, unreacted protonated Cp ligands were observed by ¹H NMR analysis of the ferrocene-containing polymer after sonication¹⁵, but were not detected in the soluble part of the cis-3FCP-containing polymer (Supplementary Fig. 26). Second, when an excess of the strong dienophile pyrenyl-maleimide was added to the sonication solution, the cross-linking did not occur (Supplementary Fig. 27) and the pyrenyl groups were attached to the polymer backbone, as characterized by triple detection (UVmultiangle light scattering-refractive index, UV-MALS-RI) gel permeation chromatography (Supplementary Figs. 28 and 29), suggesting that the Diels-Alder addition of Cp to the maleimide suppresses the cross-linking chemistry.

Conclusions

Our strategy to use conformational restriction to programme a reaction down a favoured pathway and therefore increased mechanochemical reactivity is complementary to other approaches based on changing attachment positions or intrinsic reactivity. In part as a result of this effect, FCPs themselves emerge as promising mechanophores because of mechanical susceptibilities that belie their thermodynamic stabilities, creating opportunities for their use in polymeric materials that are inert over a long time in the absence of large mechanical forces but might be quite sensitive to high loads. Incorporating lability into FCP mechanophores leads to a multifunctional response to high stresses, including an irreversible colour change that complements the transient response of popular spirocyclic-40,43-45 and dioxetane-based46,47 mechanophores. This strong spectroscopic signal depends sensitively on exogenous ligands, and it therefore can be tuned independently of the mechanophore, facilitating its use in a range of materials and detection platforms. Whereas the colourimetric response results from the release of iron, a simultaneous but independent cross-linking response results from the release of the Cp ligand, offering another handle for tailoring the multifunctional response to a given material or desired property. The production of chemically reactive and optically active species also comes with the release of substantial

stored length that can be tuned through the *ansa* bridge. Beyond the utility of the FCP architecture itself, these results suggest that the rich potential of organometallic mechanochemistry in general, and metallocene mechanochemistry in particular, should motivate further quantitative mechanistic studies that account for the large perturbations in reaction pathway that are possible under mechanical coupling.

Online content

Any methods, additional references, Nature Research reporting summaries, source data, extended data, supplementary information, acknowledgements, peer review information; details of author contributions and competing interests; and statements of data and code availability are available at https://doi.org/10.1038/s41557-020-00600-2.

Received: 25 November 2019; Accepted: 3 November 2020; Published online: 21 December 2020

References

- Akbulatov, S. & Boulatov, R. Experimental polymer mechanochemistry and its interpretational frameworks. *ChemPhysChem* 18, 1422–1450 (2017).
- Willis-Fox, N., Rognin, E., Aljohani, T. A. & Daly, R. Polymer mechanochemistry: manufacturing is now a force to be reckoned with. *Chem* 4, 2499–2537 (2018).
- Izak-Nau, E., Campagna, D., Baumann, C. & Göstl, R. Polymer mechanochemistry-enabled pericyclic reactions. *Polym. Chem.* 11, 2274–2299 (2020).
- Jung, S. & Yoon, H. J. Mechanical force induces ylide-free cycloaddition of nonscissible aziridines. *Angew. Chem. Int. Ed.* 59, 4883–4887 (2020).
- Hickenboth, C. R. et al. Biasing reaction pathways with mechanical force. Nature 446, 423–427 (2007).
- Sagara, Y. et al. Rotaxanes as mechanochromic fluorescent force transducers in polymers. J. Am. Chem. Soc. 140, 1584–1587 (2018).
- Kim, T. A., Robb, M. J., Moore, J. S., White, S. R. & Sottos, N. R. Mechanical reactivity of two different spiropyran mechanophores in polydimethylsiloxane. *Macromolecules* 51, 9177–9183 (2018).
- Lin, Y., Barbee, M. H., Chang, C.-C. & Craig, S. L. Regiochemical effects on mechanophore activation in bulk materials. *J. Am. Chem. Soc.* 140, 15060, 15075 (2018)
- Yildiz, D. et al. Anti-Stokes stress sensing: mechanochemical activation of triplet-triplet annihilation photon upconversion. *Angew. Chem. Int. Ed.* 58, 12919–12923 (2019).
- Kosuge, T. et al. Multicolor mechanochromism of a polymer/silica composite with dual distinct mechanophores. J. Am. Chem. Soc. 141, 1898–1902 (2019).
- Wang, J., Piskun, I. & Craig, S. L. Mechanochemical strengthening of a multi-mechanophore benzocyclobutene polymer. ACS Macro Lett. 4, 834–837 (2015).
- Matsuda, T., Kawakami, R., Namba, R., Nakajima, T. & Gong, J. P. Mechanoresponsive self-growing hydrogels inspired by muscle training. *Science* 363, 504–508 (2019).
- 13. Huang, W. et al. Maleimide—thiol adducts stabilized through stretching. *Nat. Chem.* **11**, 310–319 (2019).
- Chen, Z. et al. Mechanochemical unzipping of insulating polyladderene to semiconducting polyacetylene. Science 357, 475–479 (2017).
- Sha, Y. et al. Quantitative and mechanistic mechanochemistry in ferrocene dissociation. ACS Macro Lett. 7, 1174–1179 (2018).
- Di Giannantonio, M. et al. Triggered metal ion release and oxidation: ferrocene as a mechanophore in polymers. *Angew. Chem. Int. Ed.* 57, 11445–11450 (2018).
- Sha, Y. et al. Generalizing metallocene mechanochemistry to ruthenocene mechanophores. Chem. Sci. 10, 4959–4965 (2019).
- Wang, J. et al. Inducing and quantifying forbidden reactivity with single-molecule polymer mechanochemistry. Nat. Chem. 7, 323–327 (2015).
- Grandbois, M., Beyer, M., Rief, M., Clausen-Schaumann, H. & Gaub, H. E. How strong is a covalent bond? Science 283, 1727–1730 (1999).
- Kouznetsova, T. B., Wang, J. & Craig, S. L. Combined constant-force and constant-velocity single-molecule force spectroscopy of the conrotatory ring opening reaction of benzocyclobutene. *ChemPhysChem* 18, 1486–1489 (2017).
- Pill, M. F. et al. Mechanochemical cycloreversion of cyclobutane observed at the single molecule level. *Chem. Eur. J.* 22, 12034–12039 (2016).
- Schlierf, M., Li, H. & Fernandez, J. M. The unfolding kinetics of ubiquitin captured with single-molecule force-clamp techniques. *Proc. Natl Acad. Sci.* USA 101, 7299–7304 (2004).

NATURE CHEMISTRY ARTICLES

- Gossweiler, G. R., Kouznetsova, T. B. & Craig, S. L. Force-rate characterization of two spiropyran-based molecular force probes. *J. Am. Chem. Soc.* 137, 6148–6151 (2015).
- Beyer, M. K. The mechanical strength of a covalent bond calculated by density functional theory. J. Chem. Phys. 112, 7307–7312 (2000).
- Lin, Y., Kouznetsova, T. B., Chang, C.-C. & Craig, S. L. Enhanced polymer mechanical degradation through mechanochemically unveiled lactonization. *Nat. Commun.* 11, 4987 (2020).
- Lenhardt, J. M. et al. Mechanistic insights into the sonochemical activation of multimechanophore cyclopropanated polybutadiene polymers. *Macromolecules* 48, 6396–6403 (2015).
- 27. Albrecht, C. et al. DNA: a programmable force sensor. Science 301, 367–370 (2003).
- Brockwell, D. J. et al. Pulling geometry defines the mechanical resistance of a β-sheet protein. Nat. Struct. Mol. Biol. 10, 731–737 (2003).
- Bailey, A. & Mosey, N. J. Prediction of reaction barriers and force-induced instabilities under mechanochemical conditions with an approximate model: a case study of the ring opening of 1,3-cyclohexadiene. J. Chem. Phys. 136, 01B613 (2012).
- Kryger, M. J., Munaretto, A. M. & Moore, J. S. Structure–mechanochemical activity relationships for cyclobutane mechanophores. *J. Am. Chem. Soc.* 133, 18992–18998 (2011).
- Konda, S. S. M. et al. Molecular catch bonds and the anti-Hammond effect in polymer mechanochemistry. *J. Am. Chem. Soc.* 135, 12722–12729 (2013).
- Jacobs, M. J., Schneider, G. & Blank, K. G. Mechanical reversibility of strain-promoted azide-alkyne cycloaddition reactions. *Angew. Chem. Int. Ed.* 55, 2899–2902 (2016).
- Anslyn, E. V. & Dougherty, D. A. Modern Physical Organic Chemistry (Univ. Science Books, 2006).
- Bell, G. I. Models for the specific adhesion of cells to cells. Science 200, 618–627 (1978).
- Kauzmann, W. & Eyring, H. The viscous flow of large molecules. J. Am. Chem. Soc. 62, 3113–3125 (1940).

- Dudko, O. K., Hummer, G. & Szabo, A. Intrinsic rates and activation free energies from single-molecule pulling experiments. *Phys. Rev. Lett.* 96, 108101 (2006).
- Hummer, G. & Szabo, A. Kinetics from nonequilibrium single-molecule pulling experiments. *Biophys. J.* 85, 5–15 (2003).
- Hummer, G. & Szabo, A. Free energy profiles from single-molecule pulling experiments. Proc. Natl Acad. Sci. USA 107, 21441–21446 (2010).
- Gossweiler, G. R. et al. Mechanochemical activation of covalent bonds in polymers with full and repeatable macroscopic shape recovery. ACS Macro Lett. 3, 216–219 (2014).
- Robb, M. J. et al. Regioisomer-specific mechanochromism of naphthopyran in polymeric materials. J. Am. Chem. Soc. 138, 12328–12331 (2016).
- Fortune, W. & Mellon, M. Determination of iron with o-phenanthroline: a spectrophotometric study. *Ind. Eng. Chem. Anal. Ed.* 10, 60–64 (1938).
- Ramirez, A. L. B. et al. Mechanochemical strengthening of a synthetic polymer in response to typically destructive shear forces. *Nat. Chem.* 5, 757–761 (2013).
- Zhang, H. et al. Mechanochromism and mechanical-force-triggered cross-linking from a single reactive moiety incorporated into polymer chains. *Angew. Chem.* 128, 3092–3096 (2016).
- Davis, D. A. et al. Force-induced activation of covalent bonds in mechanoresponsive polymeric materials. *Nature* 459, 68–72 (2009).
- Wang, Z. et al. A novel mechanochromic and photochromic polymer film: when rhodamine joins polyurethane. Adv. Mater. 27, 6469–6474 (2015).
- Chen, Y. et al. Mechanically induced chemiluminescence from polymers incorporating a 1,2-dioxetane unit in the main chain. *Nat. Chem.* 4, 559–562 (2012).
- Clough, J. M., Balan, A., van Daal, T. L. & Sijbesma, R. P. Probing force with mechanobase-induced chemiluminescence. *Angew. Chem. Int. Ed.* 55, 1445–1449 (2016).

Publisher's note Springer Nature remains neutral with regard to jurisdictional claims in published maps and institutional affiliations.

© The Author(s), under exclusive licence to Springer Nature Limited 2020

Methods

Monomer synthesis. The FCP monomers were prepared by lithiation and carboxylation of [3] ferrocenophane and [5] ferrocenophane and subsequent esterification (Supplementary Section 2). Notably, a mixture of cis-3FCP and trans-3FCP bis-acids were obtained from the lithiation/carboxylation of [3] ferrocenophane. After esterification, the isomers of the dienes were isolated by flash column chromatography on silica gel (ethyl acetate/hexane, 1:9, as eluent). The structures were characterized by ¹H and ¹³C NMR spectroscopy (Supplementary Section 10); the spectra were consistent with previous reports ⁴⁸. Subsequent ring-closing metathesis of the dienes provided macrocyclic monomers that were suitable for copolymerization.

Polymer synthesis. Polymers with multiple mechanophores embedded along the backbone were synthesized by copolymerizing the macrocyclic mechanophore monomers with epoxy-COD by ED-ROMP. DCM was used as solvent and the monomer concentration was kept at $1-2\,\mathrm{M}$ to obtain high molecular weight polymers. The resulting polymers were precipitated three times in methanol for subsequent experiments. The synthetic procedure and characterization data are described in detail in Supplementary Section 2.

Single-molecule force spectroscopy. Dilute solutions of polymers $(0.1\text{--}1\,\mathrm{mg}\,\mathrm{ml}^{-1}$ in tetrahydrofuran) embedded with cis--3FCP, trans--3FCP or cis--5FCP were deposited on silicon substrates and dried, and then placed in an AFM fluid cell and immersed in toluene. For the constant velocity experiments, the cantilever was brought into contact with the surface and then retracted at a velocity of 300 nm s^-1. The amount of deposited polymer was adjusted so that only occasional successful pulls (less than one for every ten attempts) were obtained. Force curves with a clear, single plateau that was well separated from any detachment events were selected for analysis. The force–extension curve data were fitted according to previously published methods 49 .

Force clamping experiments were conducted and analysed as follows. Sample preparation and data collection procedures were similar to those of the constant velocity experiments. The only difference was that the instrument was programmed so that it switched into force clamp mode when it detected a 'catch' event (defined here as the pulling force reaching the threshold value of 650–800 pN for cis-3FCP and 750–900 pN for cis-5FCP, for a distance between probe and surface greater than 150 nm). The AFM stage position relative to the probe was adjusted by active feedback so as to maintain a constant 'clamp' force for up to 10s or until the polymer chain detached, whichever came first. Additional details have been published previously²⁰. The elongation of the polymer as a function of time was recorded and fitted with a single exponential decay function to obtain the force-coupled rate constant at a given force.

In all cases, we verified that the experimental changes in contour length agreed well with the expected extensions based on molecular modelling (Supplementary Table 14 and Supplementary Fig. 10), indicating the quantitative rupture of FCP units along the polymer backbone and supporting previous observations that the presence of the epoxides did not make significant contribution to the observed plateau, either through ring opening themselves or through the partial rupture of multiple attachments. Possible contributions from the rupture of multiple attachment points were also evaluated through simulation and found to be negligible sources of measurement uncertainty (Supplementary Fig. 11). We note that the calculated extension per monomer was 8.6 Å for cis-3FCP, 6.3 Å for trans-3FCP and 9.5 Å for cis-5FCP (for further details, see Supplementary Tables 10-12), much longer than those of many non-scissile mechanophores, including gem-dihalocyclopropanes^{49,50} and spiropyrans²³. Therefore, even low FCP incorporation can result in a substantial change in polymer contour length. For comparison, gem-dibromocyclopropane (gDBC)-containing polybutadiene can achieve ~30% extension with >98% gDBC content, whereas only 35% of cis-5FCP is needed to realize a similar extension⁴⁹.

Upper limit for unbridged ferrocene rupture. It is problematic, if not impossible, to unambiguously characterize the rate constant of unbridged ferrocene dissociation from SMFS experiments, because the signature of ferrocene dissociation is the loss of a bridging chain (force goes to zero), which is indistinguishable in the SMFS curves from the loss of a bridging chain through other mechanisms (that is, detachment of the chain from either surface). Nonetheless, the rate constant of bridging chain detachment can be taken as an upper limit for the rate constant of ferrocene dissociation. The rate-detachment relationship was extracted from multiple force curves using methods reported

previously, by taking the ratio of the total number of chain breaking events in a given force range to the total residence time of chains in that range (Fig. 2c and Supplementary Section 5.1)⁵¹. At forces between 1,250 and 1,400 pN, the rate constant for chain scission/detachment was determined to be $1\times10^3\,\mathrm{s}^{-1}$ (86 scission/detachment events in 0.08 s, Supplementary Fig. 2). To convert the chain detachment rate constant into a rate constant for ferrocene dissociation, we had to account for the statistical presence of ~70 ferrocenes along the average trapped, tension-bearing polymer segments. This correction led to a rate constant for ferrocene dissociation at these forces of $15\pm3\,\mathrm{s}^{-1}$ (Supplementary Fig. 2).

As discussed above, this is an upper limit for ferrocene dissociation, as the loss of the bridging chain could be due to not only ferrocene scission, but also to scission at a point other than ferrocene, such as a backbone C–C bond (although previous studies have indicated that the unbridged ferrocene is a highly selective point for mechanical scission¹⁵) and/or chain detachment from the surface. In fact, the rate constant for chain scission/detachment in the same force range for a comparable polymer without the ferrocene is $150 \, \text{s}^{-1}$ (49 scission/detachment events in 0.34 s, Supplementary Fig. 2). It is therefore likely that the force-coupled rate constant for ferrocene dissociation is less than $15 \pm 3 \, \text{s}^{-1}$, and the comparison with the BCOE mechanophore supports this contention.

Data availability

All the data generated and/or analysed during the current study are available as Supplementary Information, and the datasets supporting Fig. 2b,c through the Duke Research Data Repository (https://doi.org/10.7924/r4gq6z428).

References

- Hillman, M., Matyevich, L., Fujita, E., Jagwani, U. & McGowan, J. Bridged ferrocenes.
 Lithiation and subsequent reactions of 1,1'-trimethyleneferrocene. Organometallics 1, 1226–1229 (1982).
- Wu, D., Lenhardt, J. M., Black, A. L., Akhremitchev, B. B. & Craig, S. L. Molecular stress relief through a force-induced irreversible extension in polymer contour length. J. Am. Chem. Soc. 132, 15936–15938 (2010).
- Klukovich, H. M., Kouznetsova, T. B., Kean, Z. S., Lenhardt, J. M. & Craig, S. L. A backbone lever-arm effect enhances polymer mechanochemistry. *Nat. Chem.* 5, 110–114 (2013).
- Serpe, M. J. et al. A simple and practical spreadsheet-based method to extract single-molecule dissociation kinetics from variable loading-rate force spectroscopy data. J. Phys. Chem. C 112, 19163–19167 (2008).

Acknowledgements

The polymer synthesis, SMFS studies and mechanistic analysis formed a part of work supported by the National Science Foundation under grant no. CHE-1904016 to C.T. and S.L.C. The bulk mechanochromism and cross-linking studies formed a part of work supported by the US Army Research Laboratory and the Army Research Office under grant W911NF-15-0143 to S.L.C. In addition, C.T. acknowledges partial support from the National Science Foundation EPSCoR Program under grant no. OIA-1655740. The authors thank P. Zhang for help with the DFT calculations.

Author contributions

Y.Z. and S.L.C. conceived and designed the experiments. Y.Z., Z.W., Y.S. and Y.L. performed the synthesis. Z.W. and T.B.K. collected the AFM data. Y.Z., Z.W., T.B.K., Y.S. and C.T. analysed the data. L.S. and M.F. performed the mechanical testing. Y.S. and E.X. performed the DFT calculations. Y.Z., Y.S., C.T. and S.L.C. wrote the manuscript. All authors discussed the results and commented on the manuscript.

Competing interests

The authors declare no competing interests.

Additional information

Supplementary information is available for this paper at https://doi.org/10.1038/s41557-020-00600-2.

Correspondence and requests for materials should be addressed to S.L.C.

Peer review information *Nature Chemistry* thanks the anonymous reviewers for their contribution to the peer review of this work.

Reprints and permissions information is available at www.nature.com/reprints.